Exploiting polarization using multi-frequency SAR data and multi-dimensional time-frequency techniques

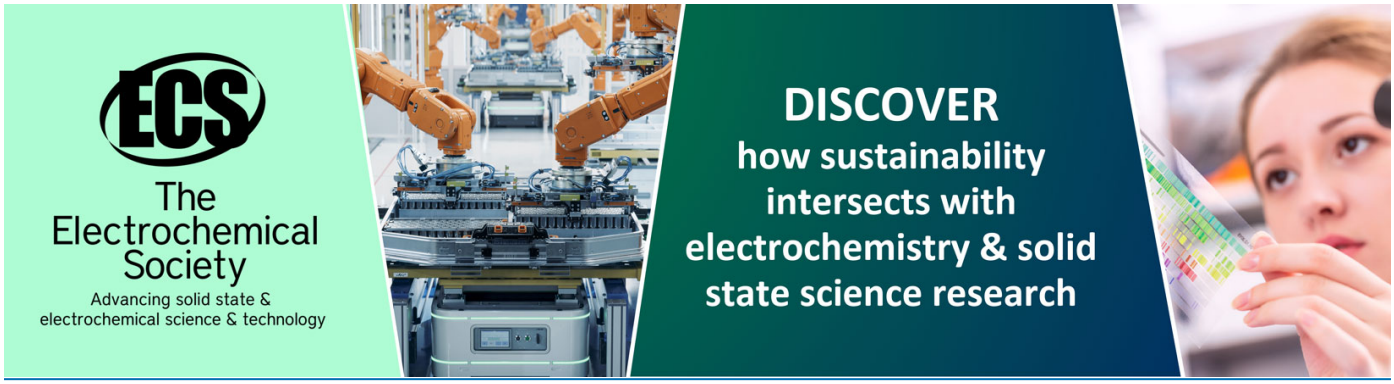

Exploiting polarization using multi-frequency SAR data and multi-dimensional time-frequency techniques

Canbin Hu[1, 2], **Wei Wang**[1], **Lingjun Zhao**[1] **and Gangyao Kuang**[1]
[1] National University of Defense Technology, College of Electronic Science and Engineering, Changsha, China
[2] University of Rennes 1, Institute of Electronics and Telecommunications of Rennes, SAPHIR team, Rennes, France

E-mail: canbinhu@gmail.com

Abstract. During recent years, Time-Frequency (TF) techniques have been introduced to characterize scene polarimetric behaviours using PolSAR data. In this paper, we apply a TF decomposition approach to the analysis of PolSAR data with different frequency bands and show some polarimetric TF behaviours of various scenes. The PolSAR data may be decomposed in azimuth direction, range direction only and in both directions. Two statistical descriptor, i.e., polarimetric TF stationarity and coherence indicators, are used to depict the features of the scene backscattering response. Their individual performance is assessed. The polarimetric TF features, extracted from the scenes of interest, can show some special relevant information compared to the original full resolution case. Moreover, with the availability of new multi-frequency full-polarization high resolution F-SAR data, the results of same site with respect to different frequency bands are exploited and compared with each other.

1. Introduction

Variations in the polarimetric properties with different azimuthal look angles and different range-frequency locations should be considered, as complex targets are illuminated from different positions and at different frequency components during SAR integration. Therefore, Time-Frequency (TF) techniques have been introduced to decompose processed PolSAR image into range-frequency and azimuth-frequency domains for characterizing scene polarimetric behaviors. In [1], a fully polarimetric subaperture analysis method was presented to describe the features of the scene backscattering response under different azimuthal look angles. In [2] [3], a two-dimensional spectral analysis, i.e., in range and azimuth, has been depicted for target detection. For remote sensing of urban areas, Schneider et al.[4] and Ferro-Famil et al.[5] characterized target polarimetric behaviors in different single direction, range and azimuth respectively.

Nowadays, many modern high-resolution SAR sensors have a wide azimuth beam width and a large bandwidth in range. Especially, the Microwaves and Radar Institute of German Aerospace Centre (DLR) has developed a new advanced airborne SAR system, the F-SAR, which can acquire data simultaneously at different wavelengths and polarizations with high range resolution. The increasing availability of new multi-frequency multi-polarization high resolution SAR data has favoured the emergence of new techniques for many different kinds of applications and permits to deal with the polarimetric characteristics of targets in more detail by means of TF techniques. In this paper, we apply a polarimetric TF decomposition approach to the analysis of F-SAR data and show the TF

behaviours of different targets and background scenes. Section 2 introduces the principle of TF decomposition method briefly and gives an overview of two statistical descriptors, i.e., polarimetric TF stationarity and coherence indicators, that can be applied to depict the features of the scene backscattering response. Experimental results are shown and discussed in section 3. The conclusions are given in section 4.

2. Polarimetric TF statistical descriptors

The first step of time-frequency analysis in azimuth, range direction or both directions is decomposition based on the use of a two-dimensional windowed Fourier transform, or 2D Gabor transform. SAR data are transformed into frequency domain at first. After correcting for spectral imbalance and multiplying by weighting function, we divide the frequency spectral band into several parts. Then each part of the spectrum is inversely transformed to the spatial domain with the representation of sub-images. After TF decomposition of PolSAR data, two indicators are introduced to measure the stationarity and coherence.

2.1. Polarimetric TF stationarity analysis

Stationarity is assessed by testing the fluctuations of the variance of the signal at different spectral locations. In full polarimetric case, a polarimetric TF scattering vector is defined by gathering the PolSAR information sampled at R spectral locations $\omega_i, i=1,\cdots,\mathrm{R}$.

$$\mathbf{k}_{\mathbf{TF}} = \left[\mathbf{k}^T(\omega_1), \cdots, \mathbf{k}^T(\omega_R)\right]^T. \tag{3}$$

where T exponent is the transpose operator, $\mathbf{k}(\omega_i)$ is a well-known scattering vector [6] :

$$\mathbf{k}(\omega_i) = \frac{1}{\sqrt{2}}\left[S_{hh}(\omega_i)+S_{vv}(\omega_i), S_{hh}(\omega_i)-S_{vv}(\omega_i), 2S_{hv}(\omega_i)\right]^T. \tag{4}$$

where $S_{pq}(\omega_i)$ represents an element of the (2×2) scattering matrix S sampled at the frequency location ω_i. A polarimetric TF sample covariance matrix, $\mathbf{T}_{\mathbf{TF\text{-}Pol}}$, is then built as follows:

$$\mathbf{T}_{\mathbf{TF\text{-}pol}} = \left\langle \mathbf{k}_{\mathbf{TF}} \mathbf{k}_{\mathbf{TF}}^{\dagger} \right\rangle = \begin{bmatrix} \mathbf{T}_{11} & \cdots & \mathbf{T}_{1R} \\ \vdots & \ddots & \vdots \\ \mathbf{T}_{R1} & \cdots & \mathbf{T}_{RR} \end{bmatrix}. \tag{5}$$

where

$$\mathbf{T}_{ij} = \left\langle \mathbf{k}(\omega_i)\mathbf{k}(\omega_j)^{\dagger} \right\rangle. \tag{6}$$

the exponent † corresponds to the transpose conjugate operator.

The signal sample variance is given by a (3×3) polarimetric coherence matrix, i.e., by the diagonal terms of the $\mathbf{T}_{\mathbf{TF\text{-}Pol}}$ matrix: $\mathbf{T}_{ii}, i=1,\cdots,R$. The polarimetric TF response is considered as stationary if the sample $\mathbf{T}_{ii}$ matrices, assumed to follow independent complex Wishart distribution $\mathbf{T}_{ii} \sim W_C(n_i, \mathbf{\Sigma}_{ii})$ with n_i looks, having the same expectation $\mathbf{\Sigma}$. The corresponding hypothesis is given by :

$$H_0 : \mathbf{\Sigma}_{ii} = \cdots = \mathbf{\Sigma}_{RR} = \mathbf{\Sigma}. \tag{7}$$

The corresponding Maximum Likelihood (ML) ratio is [1]:

$$\Lambda = \frac{\prod_{i=1}^{R} |\mathbf{T}_{ii}|^{n_i}}{|\mathbf{T}_t|^{n_t}},\ n_t = \sum_{i=1}^{R} n_i,\ \mathbf{T}_t = \frac{\sum_{i=1}^{R} n_i \mathbf{T}_{ii}}{\sum_{i=1}^{R} n_i}. \tag{8}$$

The Λ parameter with high value indicates a stationary spectral behaviour, while low value characterizes non-stationary behaviour .

2.2. Polarimetric TF coherence analysis

Coherent behaviour is defined as a phenomenon that exhibits a highly correlated behaviour over the sub-spectral. Strong and stable targets, such as corner reflectors, show high coherence. In contrast, the response from natural area may have a random behaviour and thus a low coherence. Coherence is assessed by testing the normalised correlation coefficient.

Under the hypothesis of uncorrelated spectral response, the off-diagonal terms of the TF covariance matrix equal to zero:

$$H_0 : \Sigma_{ij} = 0 \quad \forall i \neq j \,. \tag{9}$$

The corresponding ML ratio is given by:

$$\Theta = \left| \tilde{\mathbf{T}}_{\text{TF-Pol}} \right|^{n_i} . \tag{10}$$

where n_i denotes the number of looks of the sample coherency matrix, and $\tilde{\mathbf{T}}_{\text{TF-Pol}}$ is the normalized covariance matrix:

$$\tilde{\mathbf{T}}_{\text{TF-Pol}} = \begin{bmatrix} \mathbf{I} & \Gamma_{12} & \cdots & \Gamma_{1\text{R}} \\ \Gamma_{12}^{\dagger} & \mathbf{I} & & \vdots \\ \vdots & & \ddots & \vdots \\ \Gamma_{1\text{R}}^{\dagger} & \cdots & \cdots & \mathbf{I} \end{bmatrix} . \tag{11}$$

where $\Gamma_{ij} = \mathbf{T}_{ii}^{-1/2} \mathbf{T}_{ij} \mathbf{T}_{jj}^{-1/2}$.

Taking $\tilde{\mathbf{T}}_{\text{TF-Pol}}$ peculiar form into account, a correlation indicator, named TF-Pol coherence, can be defined as [5]:

$$\rho_{\text{TF-Pol}} = 1 - \left| \tilde{\mathbf{T}}_{\text{TF-Pol}} \right|^{\frac{1}{3\text{R}}} . \tag{12}$$

The TF-Pol coherence $\rho_{\text{TF-Pol}}$ reaches high values over strong coherent reflectors, such as man-made targets like ships and buildings. In contrast, the low value corresponds to natural environments.

3. Experimental results and discussion

The experimental data set used to process Time-Frequency analysis, is collected by F-SAR sensor and recorded fully polarimetric with S- and X-band on 8th June 2010 in the vicinity of Kaufbeuren, a small city in southern Bavaria, Germany. The data contains different surfaces like forest, agricultural fields, water, buildings and houses. Figure 1(a), (b) and (c) show the optical image, the Pauli basis image at S-band and the Pauli image at X-band respectively. In the Pauli-basis RGB images, the $S_{HH} + S_{VV}$ component displayed in red colour represents single (odd) bounce scattering, while $S_{HH} - S_{VV}$ in blue indicates double (even) bounce, and $S_{HV} + S_{VH}$ denoted in green colour corresponds to volume scattering. The azimuth direction is horizontal, and range is vertical increasing from top to bottom. The resolution at S-band is about 50cm in azimuth and 65cm in range direction, while it is approximately 25cm in azimuth and 25 cm in range for X-band.

3.1. TF Stationarity analysis

Figure 2 presents the log-images of the stationarity Λ parameter of the test site at both S- and X-band, obtained with 4 spectral coordinates (2 in the azimuth direction, 2 in the range direction). From the stationarity results we can observe that the Λ parameter reaches high values over natural areas, such as forests, agricultural fields and river water, indicating a stationary spectral behaviour. Over the small building area located at the top middle part of the image, Λ decreases, pointing out the invalidity of the stationary hypothesis over such complex objects. Therefore, due to the very low stationary aspect of the buildings, highly anisotropic pixels corresponding to the wall-ground dihedral reflection or

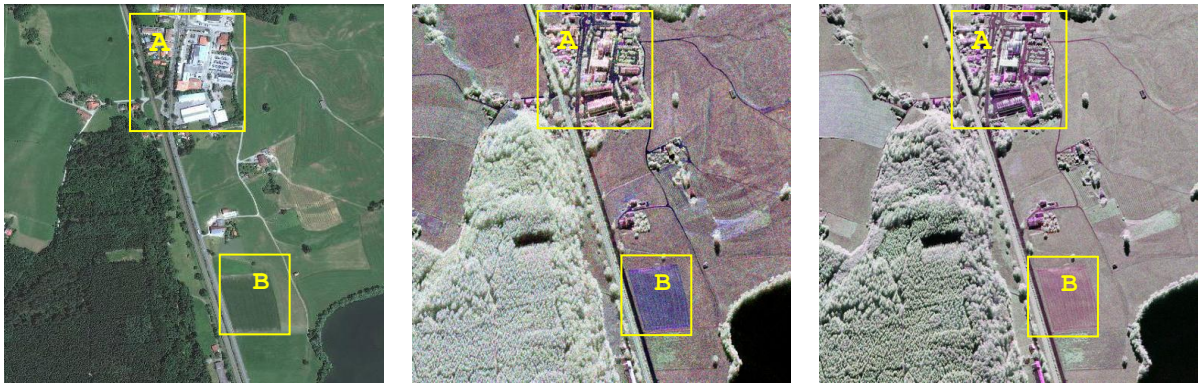

(a) (b) (c)

Figure 1. Test site of Kaufbeuren. (a) Optical image; (b) Pauli S-band image; (c) Pauli X-band image

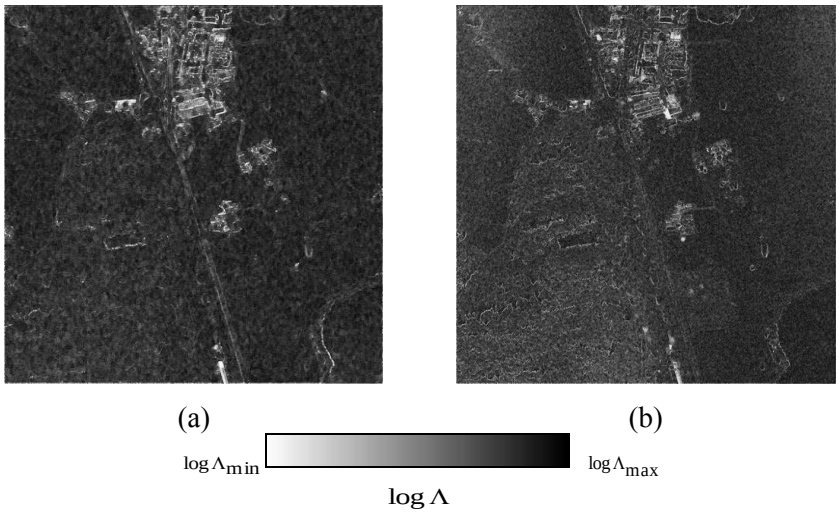

Figure 2. Stationarity ($\log \Lambda$) results. (a) S-band; (b) X-band

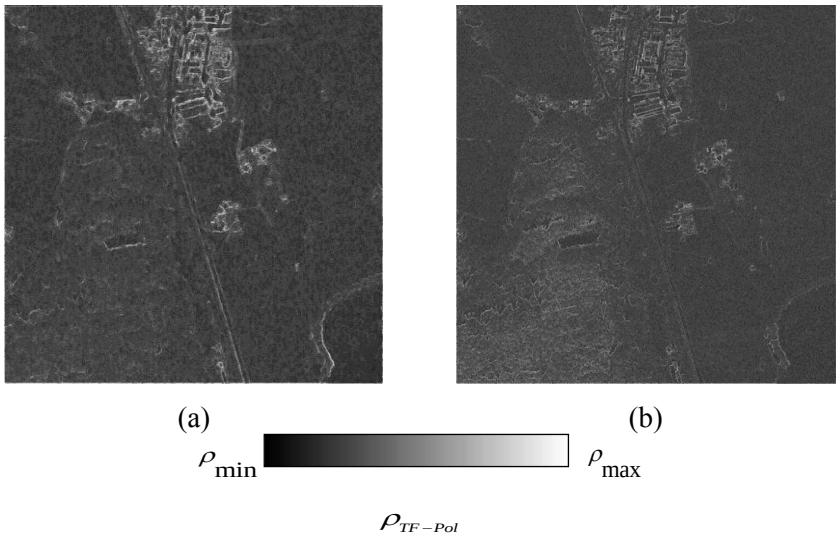

Figure 3. Coherence ($\rho_{\text{TF-Pol}}$) results. (a) S-band; (b) X-band

specular reflection from house roofs, can be clearly identified. It can be also noticed that, the forest area appears more non-stationary features at X-band than at S-band, which is expected because of the different wavelength of radar.

3.2. TF Coherence analysis

Figure 3 illustrates the TF coherence results of both frequency bands. As expected, the TF-Pol coherence is high over buildings, especially at the principal linear edges of the houses, due to the presence of strong coherent reflectors. It can be also observed that buildings are identified independently of their orientation. Comparison of the results at both bands, shows that the X-band can characterize the scenes more sophisticatedly owing to the higher resolution. Nevertheless, only few observable differences can be seen over the natural objects between the both bands.

3.3. Comparison of polarimetric information between full-resolution and TF parameters

The polarimetric parameter images at both bands are shown in Figure 4 and Figure 5. Two parameters of original full-resolution data, i.e. the entropy H and the α parameter, are obtained from the well-know Cloude-Pottier decomposition method [6]. For comparison, the two polarimetric TF indicators mentioned above, are presented again and displayed in colour bar instead of gray bar.

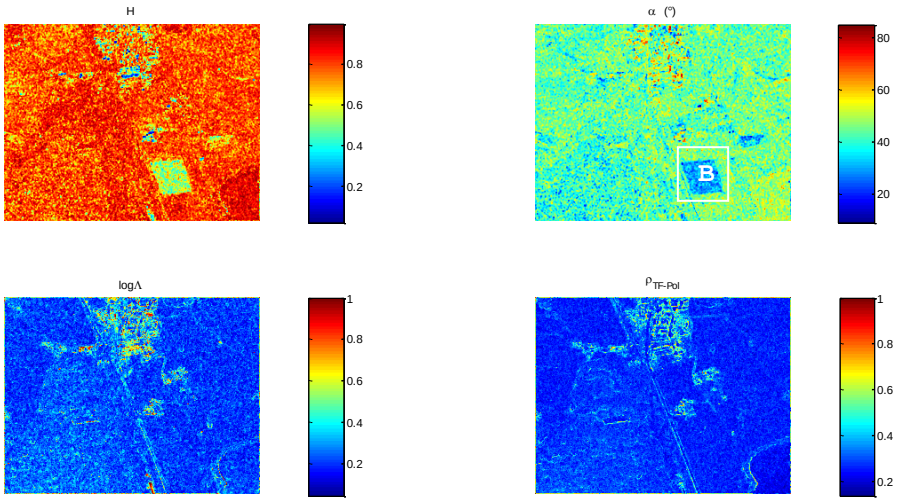

Figure 4. Polarimetric parameters at S-band

Two parts of the test site shown in Figure 1 are selected to investigate the polarimetric information. Part A is the building area, and part B is an agricultural field. Concerning the building area, it is noticed from Figure 2 and Figure 3 that these man-made targets can be discriminated from natural vegetated areas by using the polaimetric TF parameters more efficiently than the H and α indicators (see Figure 4 and Figure 5). As shown in Figure 1(b) and (c), the area B of agricultural field, reveals different scattering behaviours. At S-band, the single (odd) bounce scattering dominates this field, while the double (even) bounce scattering is prior to others at X-band. The underlying principle is that, S-band wave can penetrate this kind of agricultural crop to reach under-canopy ground by virtue of the longer wavelength, causing odd bounce scattering behaviour. However, the X-band wave is not capable of good penetration, and results in double (even) bounce reflexion with crop canopies. As shown in α parameter (area B) of Figure 4 and Figure 5, the low α value which is close to zero at S-band, and the higher α value at X-band, is consistent with the explanations above.

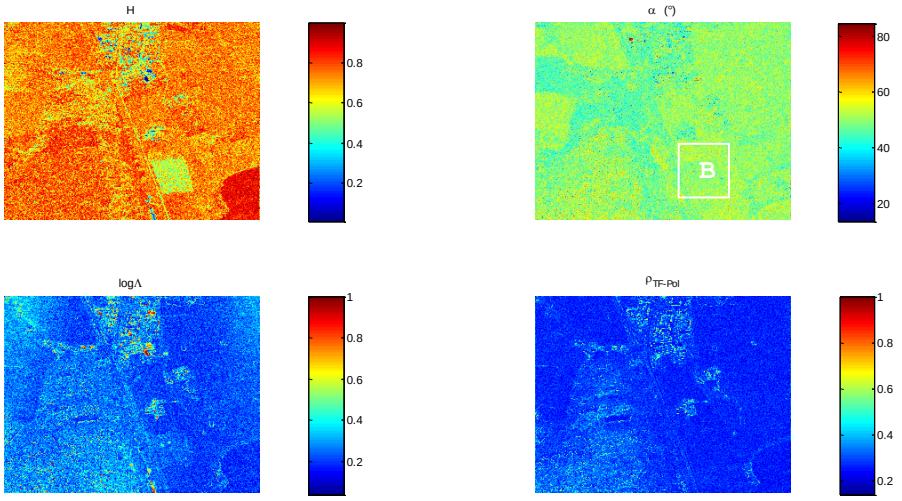

Figure 5. Polarimetric parameters at X-band

4. Conclusions

In this article, polarimetric TF diversity has been exploited with the multi-frequency band high resolution SAR data. The polarimetric parameters like entropy and α at a special crop field for different frequency bands, have been compared and analysed. It has been shown that the polarimetric TF descriptors of stationary and coherence could be efficient to characterize the response of buildings and other man-made targets. These features extracted by using multi-frequency data and TF techniques, will be combined to exploit polarization in terms of further applications (such as land terrain classification, target detection etc.) in the future work.

Acknowledgments

The authors would like to thank the DLR/F-SAR team for kindly providing F-SAR data, and the anonymous reviewers for their constructive comments and suggestions. This work was supported by the National Natural Science Foundation of China (No. 61201338).

References

[1] Ferro-Famil L, Reigber A and Pottier E 2003 Scene characterization using subaperture polarimetric sar data *IEEE Trans. Geosci. Remote Sens.* **41** 2264–76

[2] Souyris J C, Henry C and Adragna F 2003 On the use of complex sar image spectral analysis for target detection: Assessment of polarimetry *IEEE Trans. Geosci. Remote Sens.* **41** 2725–34

[3] Ferro-Famil L, Reigber A and Pottier E 2005 Nonstationary natural media analysis from polarimetric sar data using a two-dimensional time-frequency decomposition approach *Can. J. Remote Sens.* **31** 21–29

[4] Schneider R Z, Papathanassiou K, Hajnsek I and Moreira A 2006 Polarimetric and interferometric characterization of coherent scatterers in urban areas *IEEE Trans. Geosci. Remote Sens.* **44** 971–984

[5] Ferro-Famil L and Pottier E 2007 Urban area remote sensing from L-band polsar data using time-frequency techniques *Proc. IEEE Urban Remote Sens. Joint Event (Paris, France, April 2007)* pp 5045–48

[6] Cloude S R and Pottier E 1996 A review of target decomposition theorems in radar polarimetry *IEEE Trans. Geosci. Remote Sens.* **34** 498–518